

CHAPTER III

3.1. Details of the Chemicals Used

3.1.1. Solvents

Herein this dissertation various aqueous solutions were used as solvents for the research works presented. For preparing these aqueous solutions de-ionized water was collected a de-ionization plant in University of North Bengal. Next de-ionized water was doubly distilled by an all glass distilling set (as shown in Figure 3.1) with little alkaline KMnO_4 solution. The specific conductance of this doubly distilled water when checked with a Systronic Conductivity meter- 308 was $<10^{-6} \text{ S.cm}^{-1}$ at 298.15 K.¹ Required mass of solid and liquid components were mixed with necessary adjustments to have exact mass fraction of the solid component in the aqueous solvent systems.² Necessary precautions were duly taken to avoid contamination by CO_2 , moisture and other impurities. Thus the relative error in solvent composition was managed to be within 1% of the expected mass fraction. Different physico-chemical properties of these aqueous solvent systems were detailed in respective chapters.

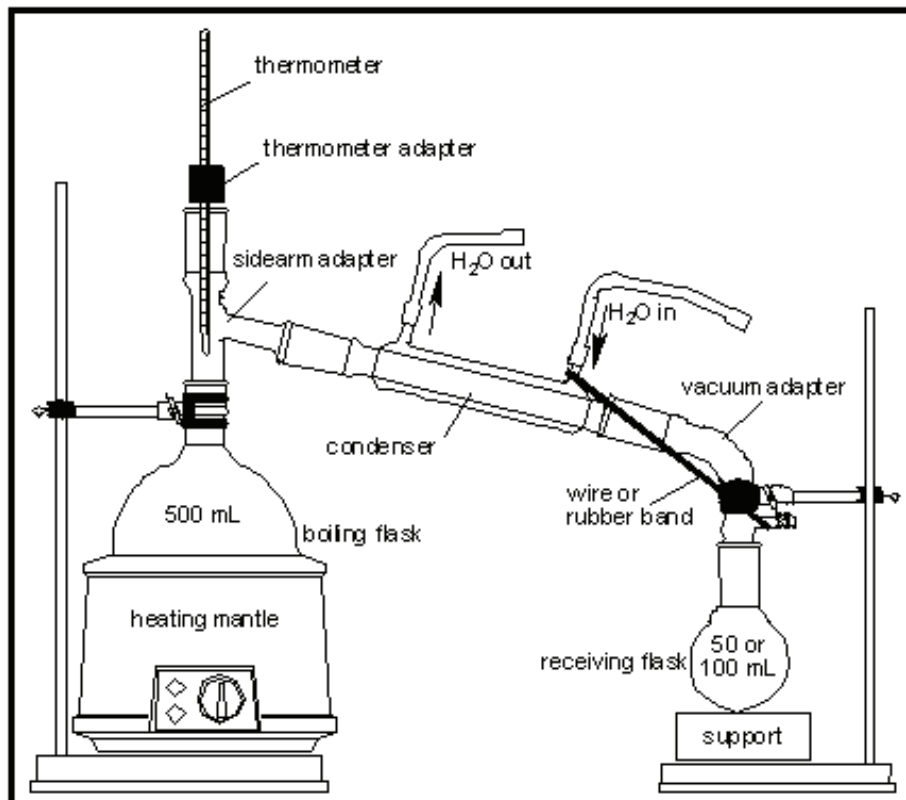


Fig 3.1. Schematic representation of the water distillation set.

Table 3.1. Details (Purity and provenance, *etc.*) of the cosolutes used.

Chemical	Source	Purification	Mass Fraction purity	CAS No
Glycine	Sigma-Aldrich, Germany	Recrystallization	>0.985	56-40-6
L-Alanine	S. D. Fine Chemicals, India	Recrystallization	>0.998	56-41-7
Sodium malonate	Sigma-Aldrich, Germany	Recrystallization	>0.970	141-95-7
Sodium gluconate	S. D. Fine Chemicals, India	None	>0.985	527-07-1
Uracil	Sigma-Aldrich, Germany	None	>0.990	66-22-8

A number of chemicals (as cosolutes) were used to make the aqueous solvent systems. Details of these cosolutes are given in Table 3.1. Glycine and L-alanine were purified by recrystallization from hot distilled water at 90-95 °C. After filtration, the residues were dehydrated in *vacuo* for several hours. The melting points of glycine and L-alanine were recorded through open capillary method to be 233 and 258 °C,^{3,4} respectively. However, uracil was used as procured from the commercial source but before use it was dried over anhydrous CaCl₂ in *vacuo* for several hours. Sodium malonate was recrystallized from ethanol and then dried carefully in *vacuo* for few hours before work.⁵ Sodium gluconate was used as purchased from the commercial sources without any purification.

3.1.2. Solutes

A number of biologically important compounds were used as solutes for research works represented in this dissertation. Stock solutions of these solutes in different aqueous solvent systems were made by mass and the different working solutions for subsequent physico-chemical studies were prepared by mass dilution. Molalities (*m*) of solutes were transformed into corresponding molarities (*c*) by use of experimental densities. All solutions were made ready afresh with adequate precautions to avoid any contamination and then degassed by dry nitrogen. The

Experimental Section

uncertainty of molality (c) of the solutes in solutions was found as $\pm 0.001 \text{ mol.kg}^{-1}$. Details of these solutes are given in Table 3.2.

Table 3.2. Details (Purity and provenance, *etc.*) of the solutes used.

Chemical*	Purification	Mass fraction purity	CAS No
L-ascorbic acid	None	>0.990	50-81-7
Nicotinic acid	None	>0.995	59-67-6
Paracetamol	None	>0.990	103-90-2
Sodium pyruvate	None	>0.985	590-46-5
Caffeine	None	>0.990	58-08-2

*Source: Sigma-Aldrich, Germany.

L-ascorbic acid, paracetamol, sodium pyruvate were not purified further but they were dried in *vacuo* through anhydrous CaCl_2 for hours before its use. Nicotinic acid was utilized as given by the vendor and melting point of nicotinic acid was recorded as to be $261 \text{ }^\circ\text{C}$.³

3.2. Experimental Methods

3.2.1. Mass measurement

Mass measurements of the solutes and cosolutes were performed by a digital analytical electronic balance (Mettler Toledo, Switzerland, AG 285) depicted in Figure 3.2.



Fig 3.2. Mettler Toledo digital balance, Switzerland, Model-AG 285.

Experimental Section

In this balance the weighing pan is inside a crystal clear enclosure with doors to operate to avoid any dust particles gathering and disturbances from any air currents. It measures masses with very high precision and accuracy (mass measurements accurate to ± 0.01 mg).

3.2.2. Density measurement

Densities of different experimental aqueous solvent systems and the working solutions were measured at the experimental temperatures with the aid of a digital density meter (Anton Paar, DMA-4500M). Figures 3.3-3.6 depict the density meter, its display, sample filling and cell drying, respectively.



Fig 3.3. Anton Paar density meter (DMA-4500M).



Fig 3.4. Display of Anton Paar density meter.

Experimental Section



Fig 3.5. Filling of sample with a syringe.



Fig 3.6. Drying the measuring cell.

The mechanical oscillation of the U-tube of this density meter is electromagnetically converted into an alternating voltage with the same frequency. The oscillation period (τ_0) is exactly computed with high resolution and there is a simple correlation between the oscillation period (τ_0) and the density (ρ) of the studied sample as given by the relation:⁶

$$\rho = A\tau_0^2 - B \quad (1)$$

where A and B stand for the instrument constants that can be obtained through calibration with two liquids of precisely known densities. The densities of these two liquids must be different by at least $\pm 0.01 \text{ g} \cdot \text{cm}^{-3}$ and values of τ_0 of the adjustment media must be different by at least 0.0001 unit. Modern and modified instruments can compute and store the A and B constants after calibration, mostly performed with water and air. For the various experiments, however, the density meter was previously calibrated with doubly distilled de-ionized degassed water and dry air at the various experimental temperatures under atmospheric pressure. In this instrument the

Experimental Section

temperature is maintained at the experimental temperatures with an accuracy of $\pm 1 \times 10^{-2}$ K with an automatic built-in Peltier technique. The stated repeatability and accuracy of the densities are $\pm 1 \times 10^{-5} \text{ g} \cdot \text{cm}^{-3}$ and $\pm 5 \times 10^{-5} \text{ g} \cdot \text{cm}^{-3}$, respectively. But when the accuracy of the densities of the experimental solutions was compared to the densities of a known molal aqueous NaCl solution using the data given by Pitzer,⁷ the estimated uncertainty of the densities for most of the solutions was found to be better than $\pm 2 \times 10^{-5} \text{ g cm}^{-3}$.

3.2.3. Viscosity measurement

The kinematic viscosities were determined by a suspended-level Cannon type Ubbelohde viscometer (capillary type). The time of efflux of a constant volume liquid sample through the capillary was measured with a digital stopwatch with a time accuracy of ± 0.01 s. The viscometer was always kept vertically immersed in the thermostatic bath maintained at the experimental temperature ± 0.01 K. After some time when the thermal equilibrium was established, the flow times of the samples were measured thrice and the average of all these readings were taken into account for the determination of viscosity. During the measurements necessary precautions were adopted to avoid evaporation losses and any contamination. The efflux time for water at temperature 298.15 K was measured as 428.9 s. The kinematic viscosity (ν) and the absolute viscosity (η) are obtained using the relations:⁸

$$\nu = kt - \frac{L}{t} \quad (2)$$

$$\eta = \nu\rho \quad (3)$$

where k and L are the characteristic viscometer constants; t and ρ stand for the efflux time of flow in seconds and sample density, respectively. The calibration constants (k and L) were determined with purified water and methanol and they were found to be 1.9602×10^{-3} and 4.2019, respectively. Of note is the fact that the kinetic energy corrections were found to be almost negligible and the uncertainty of viscosities was within $\pm 4 \times 10^{-4} \text{ mPa} \cdot \text{s}$ based on our recent measurements on different pure liquids. Figure 3.7 depicts the suspended-level Cannon type Ubbelohde viscometer (capillary type) used.

Experimental Section

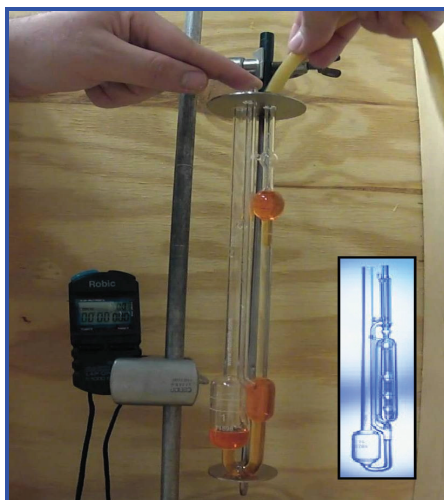


Fig 3.7. A suspended-level Cannon type Ubbelohde viscometer (capillary type).

3.2.4. Refractive index measurement

Refractive indices of the experimental liquid samples were determined with the aid of a Abbe-refractometer (Cyberlab, MA01527, USA) using sodium D-line light ($\lambda=589.3$ nm, an average of the two emission lines at 589.0 nm and 589.6 nm) at 298.15 K. The Abbe-refractometer is one of the most acceptable and extensively used refractometer and it has the range ($n_D = 1.3$ to 1.7). Figure 3.8 schematically depicts this optical system. The sample liquid is directly placed in the prism assembly of the instrument using an airtight hypodermic syringe and is sandwiched like a skinny film (~ 0.1 mm) between the two prisms. The upper prism is solidly framed on a bearing that permits its rotation through the side arm presented by dotted lines. The lower prism is hooked to the upper prism to empower separation for washing and for the introduction of the particular sample. When light reflects into the prism, the lower surface being rough is converted to origin for the endless number of rays that transits along the sample at all angles.

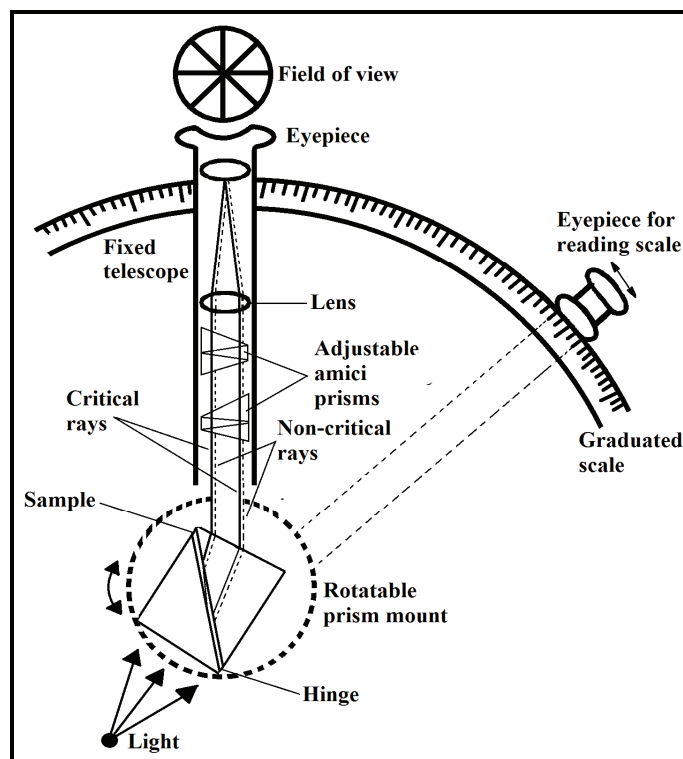


Fig 3.8. Schematic illustration of the Abbe-refractometer optical system.

The light rays are refracted at the smooth-ground face and interface of the upper prism and sample, respectively. Then it transits along a fixed telescope. Divergent rays of several colors are combined into a single white beam by two triangular prisms in contact (Amici prisms). The beam conforms almost exactly in the path to that of sodium D-ray. The eyepiece is marked with crosshairs in the telescope (Figure 3.8). During the determination of the refractive index the angle of the prism is altered until the light-dark interface just coexists with the crosshairs. Then the prism position is read from the locked scale. An average of three numbers of measurements was taken for each mixture. The Abbe-refractometer is shown in Figure 3.9. During the determination, water from a thermostatic bath maintained at 298.15 ± 0.01 K was transmitted along the refractometer and it was calibrated by determining the refractive indices of doubly distilled de-ionized degassed water at temperature 298.15 K. The uncertainty in refractive indices was within ± 0.0002 .

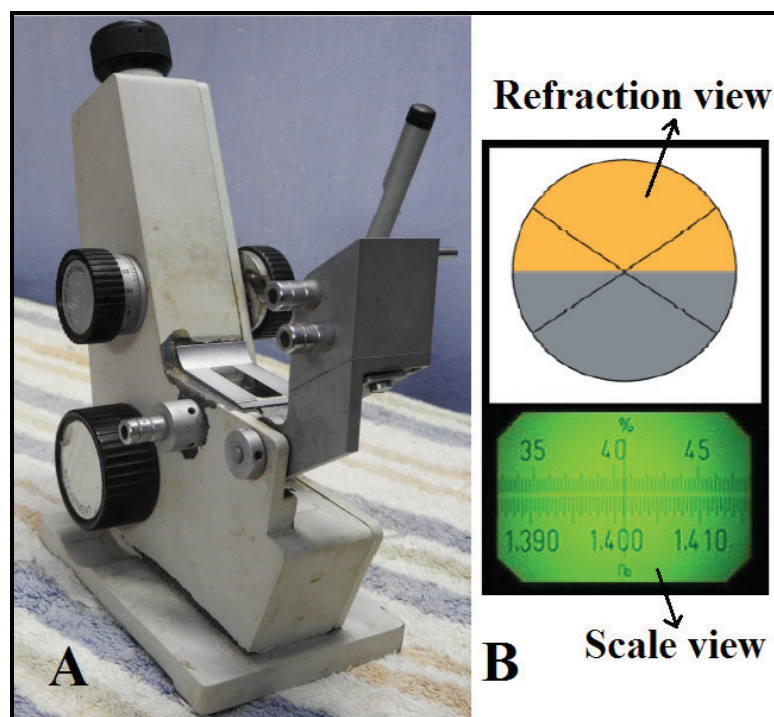


Fig 3.9. A: Abbe-refractometer (Cyberlab, MA01527, USA); B: View of the refractometer through the eyepiece.

3.2.5. Spectrophotometric measurements

Absorption spectra of biologically important compounds used as solutes in various aqueous media were recorded on a Jasco V-530 double beam UV-VIS spectrophotometer at 298.15 K. Figure 3.10 shows the UV-VIS Spectrophotometer. It was fitted with a thermostatic arrangement to maintain a temperature of 298.15 ± 0.01 K. Quartz cells of 1 cm path length were used to hold the samples and the reference solvents during the spectral measurements. A stock solution of biologically important samples was prepared in the aqueous solvent systems and 2 mL of it was taken in the quartz cell and measurement of absorption was done against a selected reference solvent system. Then solution of co-solute (of fixed concentration) in the reference solvent or in an aqueous solvent was added stepwise by using a pre-calibrated Hamilton syringe. After 30 seconds the absorbance of the resulting solution was measured at each step.



Fig 3.10. Double beam UV-VIS Spectrophotometer (Jasco V-530) and the thermostatic bath.

3.2.6. Ultrasonic Velocity Measurements

Three types of experimental techniques are available to determine the ultrasonic sound velocities in liquid mixtures and pure liquids. They are: (i) Pulse method, (ii) Continuous wave method and (iii) Interferometer technique. From a comparison of the comparative merits of the different methods, interferometer method is found to be the most accurate method available for speed measurements. Hunter and Dardy,⁹ Dobbs and Fine gold,¹⁰ Fort and Moore¹¹ measured the speed of sound for liquids and liquid mixtures by using interferometric technique with $\pm 0.15\%$ uncertainty. Herein the present research work ultrasonic speeds of the experimental liquid samples were recorded with an exactness of 0.3% using a multi-frequency ultrasonic interferometer (F-05, Mittal Enterprises; New Delhi, India) operating at 2 MHz. It was calibrated with purified benzene, doubly distilled de-ionized degassed water maintained at 298.15 ± 0.01 K by circulating thermostatic water around the jacketed cell (of 2 MHz) containing the liquid sample by a circulating pump. The uncertainty in ultrasonic speeds was around $\pm 0.2 \text{ m s}^{-1}$.

The measurement of ultrasonic speed (u) by ultrasonic interferometer is dependent on the exact calculation of wavelength (λ) in the medium. In this process ultrasonic waves of noted frequency (f) are generated by a crystal of quartz hooked at the bottom part of the cell. These ultrasonic waves are reflected by a transportable plate of metal (maintained parallel to the quartz crystal). When the interspace amongst these two plates becomes a whole multiple of the wavelength of ultrasonic sound, the

Experimental Section

standing waves are produced in that medium. In this situation, acoustic resonance is generated. The acoustic resonance forms an electrical reaction in the generator that drives the quartz crystal and as a result the current of anode in the generator reaches the maximum level. When the distance is enlarged or diminished by accurately one half of the wavelength ($\lambda/2$) or an integer multiple of the wavelength, the current of anode again reaches the maximum level. If d is the separation between consecutive adjoining maxima of current of anode and the full number of oscillation (usually $n = 20$) counted. Then the total distance moved by the micrometer in n oscillations is given by:

$$d = n \times \frac{\lambda}{2} \quad (4)$$

Now the speed (u) of the wave and frequency (f) of the cell is related to its wavelength (λ) by the relation,

$$u = \lambda \times f \quad (5)$$

$$\text{Or } u = \lambda \times f = \frac{2d}{n} \times f \quad (6)$$

Thus with a known cell frequency the ultrasonic speed (u) can be obtained. The ultrasonic interferometer has the three main portions: (i) The high frequency generator (single and multi-frequency) is specially outlined to excite the crystal of quartz hooked at the bottom part of the measuring cell. Its resonant frequency is served for generation of ultrasonic wave in the studied liquid filled in the measuring cell, (ii) shielded cable and (iii) The measuring cell (1, 2, 3 and 4 MHz) is specially drafted with double walled cell which maintains the temperature of the sample liquid constant during the whole process. To raise or lower the reflector plate in the liquid a fine micrometer has been applied. It is arranged at the top in the cell and works through a known gap.

The total assembly is shown Figure 3.11 in which the output terminal of that high frequency generator is anchored with the measuring cell by a shielded cable. At first the cell is filled with the experimental liquid and then the switch of the generator is made on. It is normally observed that the ultrasonic waves generally move normal from the crystal of quartz crystal until they are reflected back by the portable plate and the standing waves are generated in liquid in between the quartz crystal and the

Experimental Section

reflector plate. Next the micrometer proceeds slowly till the anode current exhibits a maximum deflection on the meter of the high frequency generator. A number of maxima of current of anode are observed and the whole number of oscillation (n) is computed. The total space (d) thus moved by the micrometer provides the wavelength (λ) using the Eq. (4).

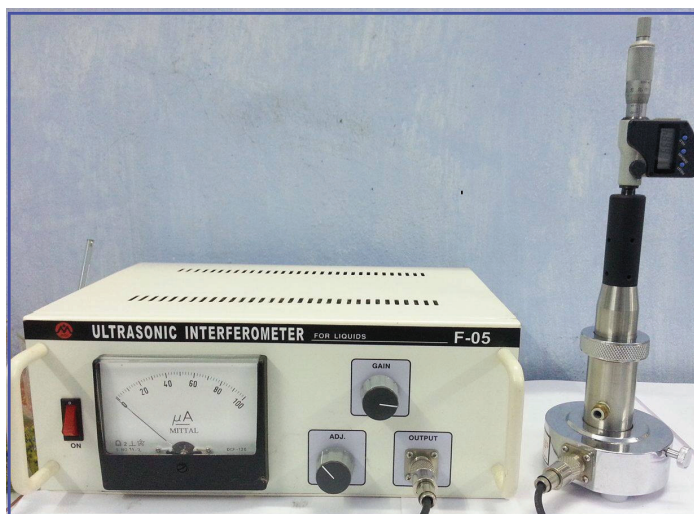


Fig 3.11. Ultrasonic interferometer (F-05, Mittal Enterprises, India).

In Fig. 3.12 a cross-section of the measuring cell of ultrasonic interferometer with multi-frequency and position of reflector *versus* crystal current are shown. The extra peaks [appearing in Figure 3.12 B] in between minima and maxima occur due to a number of reasons but these do not influence on the $\lambda/2$ values.

3.2.7. pH Measurements

A Systronics digital pH meter was used to record the pH's of the experimental solutions. Before use it was calibrated at pH = 4.00 using buffer capsule of pH = 4.00 (procured from Sigma-Aldrich, Germany). Figure 3.13 illustrates the Systronics digital pH meter used.

Experimental Section

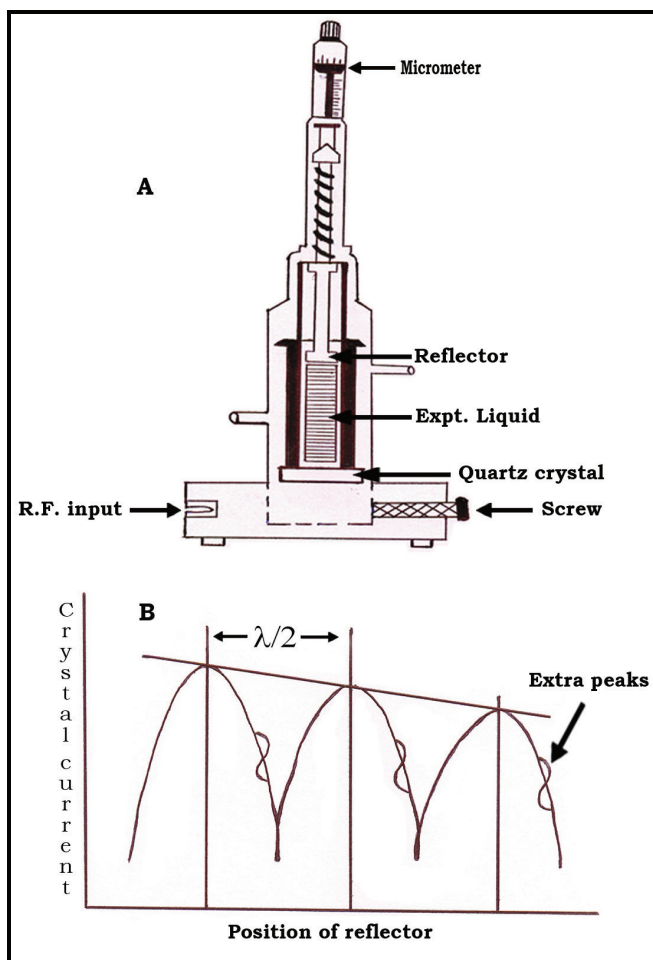


Fig 3.12. (A) A cross-section of the measuring cell of a multi-frequency ultrasonic interferometer; (B) position of reflector *versus* crystal current.



Fig 3.13. Systronics digital pH meter.

References

- [1] D. Brahman, B. Sinha, *J. Chem. Eng. Data* 56 (2011) 3073-3082.
- [2] A. Sarkar, B. K. Pandit, B. Sinha, *J. Chem. Thermodyn.* 98 (2016) 118-125.
- [3] A. Sarkar, B. Sinha, *J. Serb. Chem. Soc.* 78 (8) (2013) 1225-1240.
- [4] B. Sinha, A. Sarkar, P. K. Roy, D. Brahman, *Int. J. Thermophys.* 32 (2011) 2062-2078.
- [5] I. J. Warke, K. J. Patil, S. S. Terdale, *J. Chem. Thermodyn.* 93 (2016) 101-114.
- [6] Oscillating U-tube. Electronic document,
http://en.m.wikipedia.org/wiki/Oscillating_U-tube, accessed on Oct 12, 2013.
- [7] K. S. Pitzer, J. C. Peiper, R. H. Busey, *J. Phys. Chem. Ref. Data* 13 (1984) 1-102.
- [8] T. S. Banipal, H. Singh, P. K. Banipal, V. Singh, *Thermochimica Acta.* 553 (2013) 31-39.
- [9] Y. L. Hunter, H. D. Dardy, *J. Acoust. Soc. Amer.* 36 (1964) 1914.
- [10] E. R. Dobbs, L. Finegold, *Ibid*, 32 (1960) 1215.
- [11] R. J. Fort, W. R. Moore, *Trans Faraday Soc.* 61 (1965) 2102.